JOURNAL OF BACTERIOLOGY, Jan. 1991, p. 575–586
0021-9193/91/020575-12$02.00/0

Vol. 173, No. 2

Genetic and Transcriptional Organization of the *hrp* Cluster of *Pseudomonas syringae* pv. phaseolicola

LAURENCE G. RAHME, MICHAEL N. MINDRINOS,† AND NICKOLAS J. PANOPOULOS*
Department of Plant Pathology, University of California, Berkeley, California 94720

Received 23 July 1990/Accepted 19 October 1990

The *hrp* cluster of *Pseudomonas syringae* pv. phaseolicola encodes functions that are essential for pathogenicity on bean plants and for the elicitation of the hypersensitive response on resistant plants. The cluster was saturated with insertions of transposon Tn*3*-spice that served both as a mutagen and as a sensitive reporter of the expression of the target regions. The mutations covered a 17.5-kb segment in strain NPS3121, in which seven *hrp*::Tn*5* insertions had been previously mapped, and regions outside this segment. The cluster is organized into seven distinct complementation groups (*hrpL*, *hrpAB*, *hrpC*, *hrpD*, *hrpE*, *hrpF*, and *hrpSR*) on the basis of the analysis of over 100 Tn*3*-spice insertions in plasmids and 43 similar insertions in the chromosome; it spans nearly 22 kb and is chromosomally located. The transcriptional orientation of all genes in the cluster was established by measuring the level of ice nucleation activity of complemented merodiploids carrying chromosomal *hrp*::*inaZ* fusions after inoculation in Red Kidney bean leaves. Although all seven loci were actively expressed in Red Kidney bean leaves, none of them was substantially expressed when the bacteria were grown in King B broth medium. Mutations in all loci, except those in *hrpC*, greatly reduced the ability of the bacteria to multiply in bean leaves. Mutations in the *hrpC* locus, although preventing the bacteria from eliciting a hypersensitive reaction on tobacco, allowed the bacteria to produce delayed and attenuated symptoms in Red Kidney bean leaves and to multiply to a level 10^2- to 10^3-fold lower than that of the wild-type strain. This is the first comprehensive report of the genetic and transcriptional organization of the *hrp* gene cluster in a phytopathogenic bacterium.

The bean halo blight pathogen, *Pseudomonas syringae* pv. phaseolicola, possesses a group of genes, designated *hrp* ("harp"), that are essential for the development of disease symptoms and for the elicitation of the hypersensitive reaction on resistant plants. The majority of known *hrp* genes in this bacterium are clustered in a large genomic region that has been designated the *hrp* cluster, whereas one locus (*hrpM*) is located elsewhere in the genome (24, 29, 31, 36). Besides *P. syringae* pv. phaseolicola, *hrp* genes and/or gene clusters from several other members of the *P. syringae* taxon have been described and cloned (5, 13–16, 24, 30, 33, 37–39), as have those from phylogenetically distinct plant pathogens, such as *Pseudomonas solanacearum* (2, 14), *Erwinia amylovora* (44, 45), and some pathovars of *Xanthomonas campestris* (2, 6, 42). Homology between *hrp* genes has been reported among members of the *P. syringae* taxon (8a, 24) as well as between *P. solanacearum* and members of the *X. campestris* group (2).

The nature and precise role of most *hrp* gene products in the plant-bacterium interaction are unknown. Three *hrp* loci have been analyzed in some detail in *P. syringae* pv. phaseolicola. A locus designated *hrpS* encodes a protein that shares sequence similarity to NtrC-like regulatory proteins (10–12). Another locus, designated *hrpD*, is actively expressed at early stages of infection (8c, 23) and requires a functional *hrpS* gene to be expressed (10, 11, 30). A third locus, *hrpM*, is capable of coding for two polypeptides (40 and 82 kDa) that are predicted to be integral membrane proteins with a possible role in transport (8a). A similar role was suggested for the *hrpM* homolog of *P. syringae* pv. syringae (29, 31). Finally, a role in the regulation of the expression of an avirulence gene (*avrB*) and in integrating information about carbon source availability was proposed for genes that are located at the ends of the *hrp* cluster of *P. syringae* pv. glycinea (16).

Although mutational analysis of *hrp* clusters from *P. syringae* pv. phaseolicola and other phytopathogenic bacteria has been carried out (2, 16, 24, 30, 31, 36), none of these regions has been fully characterized in respect to its overall genetic organization, such as the number of complementation groups and the transcriptional orientation of the various genes.

The objectives of the present study were to (i) saturate the entire *hrp* cluster of *P. syringae* pv. phaseolicola with reporter insertions, (ii) analyze the mutations for their phenotypic effect on the bacterium-host and bacterium-nonhost interactions, (iii) establish the genetic and transcriptional organization of the cluster, and (iv) determine the ability of *hrp* mutants representing each distinct complementation group to multiply in the leaves of a susceptible host. Since the *hrp* cluster of *P. solanacearum* (2), the virulence and tumor-inducing genes of *Agrobacterium* spp. (32), and the symbiotic gene clusters of *Rhizobium* spp. (27) are located on large plasmids, we also investigated whether the *hrp* cluster of *P. syringae* pv. phaseolicola might be located on extrachromosomal elements.

(Preliminary results of these studies have been presented elsewhere [30, 36].)

MATERIALS AND METHODS

Media, reagents, and growth conditions. *Escherichia coli* strains were grown in Luria-Bertani (LB) medium (26) at 37°C. *P. syringae* pv. phaseolicola strains were grown in King B (KB) medium (19), normally at 28°C. In experiments

* Corresponding author.
† Present address: Department of Molecular Biology, Massachusetts General Hospital, Boston, MA 02114.

TABLE 1. Bacterial strains and plasmids[a]

Strain or plasmid	Relevant properties	Source or reference
Escherichia coli		
HB101	F$^-$ *hsdS20* (*hsdR hsdM*) *recA13 thi leu arg-14 proA2 lacY1 galK2 rpsL xyl-5 mtl-1 supE44* λ^-	
DH5α	F$^-$ *endA1 hsdR17*(r_K^- m_K^+) *supE44 thi recA1 gyrA* φ80*lacZ*ΔM15 *relA1* Δ(*lac-proAB-argF*) λ^-	Bethesda Research Laboratories
SF800	Nal^r *polA*(Ts) *thy*	W. Paranchych
Pseudomonas syringae pv. phaseolicola		
NPS3121	Wild type, Rif^r	
NPS4000	NPS3121 *hrpA4000*::Tn*5*	24
NPS4002	NPS3121 *hrpD4002*::Tn*5*	24
NPS4004	NPS3121 *hrpD4004*::Tn*5*	24
NPS4007	NPS3121 *hrpE4007*::Tn*5*	24
NPS4001	NPS3121 *hrpE4001*::Tn*5*	24
NPS4003	NPS3121 *hrpF4003*::Tn*5*	24
NPS4006	NPS3121 *hrpS4006*::Tn*5*	24
LRB1011	NPS3121 *chr1011*::Tn*3*-spice	This study
LRB1013	NPS3121 *chr1013*::Tn*3*-spice	This study
LRB210	NPS3121 *chr210*::Tn*3*-spice	This study
LRD410	NPS3121 *chr410*::Tn*3*-spice	This study
LRE613	NPS3121 *hrpL613*::Tn*3*-spice	This study
LRE813	NPS3121 *chr813*::Tn*3*-spice	This study
LR72	NPS3121 *hrpB72*::Tn*3*-spice	This study
LR323	NPS3121 *hrpB323*::Tn*3*-spice	This study
LR42	NPS3121 *hrpB42*::Tn*3*-spice	This study
LR71	NPS3121 *hrpB71*::Tn*3*-spice	This study
LR348	NPS3121 *hrpB348*::Tn*3*-spice	This study
LR70	NPS3121 *hrpB70*::Tn*3*-spice	This study
LR413	NPS3121 *hrpB413*::Tn*3*-spice	This study
LR2	NPS3121 *hrpB2*::Tn*3*-spice	This study
LR328	NPS3121 *hrpB328*::Tn*3*-spice	This study
LR38	NPS3121 *hrpC38*::Tn*3*-spice	This study
LR62	NPS3121 *hrpC62*::Tn*3*-spice	This study
LR50	NPS3121 *hrpD50*::Tn*3*-spice	This study
LR12	NPS3121 *hrpB12*::Tn*3*-spice	This study
LR57	NPS3121 *hrpB57*::Tn*3*-spice	This study
LR6	NPS3121 *hrpB6*::Tn*3*-spice	This study
LR65	NPS3121 *hrpB65*::Tn*3*-spice	This study
LRB42	NPS3121 *chr42*::Tn*3*-spice	This study
LR7	NPS3121 *chr7*::Tn*3*-spice	This study
LR5	NPS3121 *chr5*::Tn*3*-spice	This study
LR33	NPS3121 *hrpF33*::Tn*3*-spice	This study
LR66	NPS3121 *hrpF66*::Tn*3*-spice	This study
LRA11	NPS3121 *hrpF11*::Tn*3*-spice	This study
LRE44	NPS3121 *hrpE44*::Tn*3*-spice	This study
LR64	NPS3121 *hrpF64*::Tn*3*-spice	This study
LRD71	NPS3121 *hrpF71*::Tn*3*-spice	This study
LRB63	NPS3121 *hrpF63*::Tn*3*-spice	This study
LRA102	NPS3121 *hrpF102*::Tn*3*-spice	This study
LR8	NPS3121 *hrpF8*::Tn*3*-spice	This study
LR4	NPS3121 *hrpF4*::Tn*3*-spice	This study
LRG94	NPS3121 *hrpS94*::Tn*3*-spice	This study
LRB14	NPS3121 *hrpR14*::Tn*3*-spice	This study
LRH122	NPS3121 *hrpR122*::Tn*3*-spice	This study
LRC124	NPS3121 *hrpR124*::Tn*3*-spice	This study
LRB24	NPS3121 *chr24*::Tn*3*-spice	This study
LRA32	NPS3121 *chr32*::Tn*3*-spice	This study
LRB104	NPS3121 *chr104*::Tn*3*-spice	This study
Plasmids		
pLAFR3	Broad-host-range vector, *incP-1* rlx_{RK2}^+ rep_{RK2}^+ *lacZ*α *cos*$^+$, Tet^r	43
pLAFR6	As pLAFR3 but without *lacZ*α, contains the multilinker of pUC18 flanked by synthetic *trp* terminators, Tet^r	16
pLAFR6-*inaZ*	pLAFR6 carrying the *P. syringae* ice nucleation gene (*inaZ*) from nucleotide 775 to 4458	9, 16, 22
pPL6, pPL3, pNN56	*hrp* cosmid clones	24; this study
pPL1	pLAFR3 cosmid carrying the Tn*5* and flanking sequences from NPS4000	23

Continued on following page

TABLE 1—*Continued*

Strain or plasmid	Relevant properties	Source or reference
pPL11	Carries the 20-kb *Bam*HI-*Hin*dIII fragment of the *hrp* cluster inserted in the synonymous sites of the broad host range vector pWB5A, Tet^r	22
pLRBR	Carries the 9.3-kb *Bam*HI-*Eco*RI fragment from p7 cloned in pLAFR6	This study
pMM6AS	Carries the 6.3 kb *Sac*I fragment cloned in pLAFR6	This study
pMM3AS	Carries the 6.3-kb *Sac*I fragment cloned in pLAFR3	This study
pMM6AS2	As pMM6AS but with a 0.6-kb *Eco*RV-*Sac*I extension	This study
pMM18	Carries the 2.1-kb *Bam*HI fragment cloned in pLAFR6-*inaZ*	This study
pLR32	Carries the 3.6-kb *Bgl*II fragment cloned in pLAFR6	This study
pLR86	Carries the rightmost 1.8-kb *Pst*I-*Bst*EII segment of the pLR32 insert cloned in pLAFR6-*inaZ*	This study
pTn*3*-spice	pMB8 replicon, carries tranposon Tn*3*-spice, Tet^r Spc^r Str^r	(22, 41)
pRK2013	rep_{E1}^+ Δrep_{RK2} tra_{RK2}^+ rlx_{RK2}^+, Kan^r	8
BLUESCRIBE(+)	Amp^r	Vector Cloning Systems, San Diego, Calif.
pGEM-7Zf(+)	Amp^r	Promega Corp., Madison, Wis.
pIBI76	Amp^r	International Biotechnologies, Inc., New Haven, Conn.
pB1011, pB1013, pB210, pD410, pE613, PE813	pPL3::Tn*3*-spice derivatives (Fig. 2)	This study
pB53, pB42, pC52, pH48, pA11, pF94, pE44, pA34, pD71, pH84, pB63, pA102, pG94, pB14, pH122, pC124, pH94, pA21, pB24, pA32, pB104	pNN56::Tn*3*-spice derivatives (Fig. 4)	This study
p72, p44, p46, p323, p45, p48, p42, p713, p348, p70, p413, p52, p69, p2, p68, p328, p38, p62, p50, p12, p57, p6, p65, p7, p5, p33, p66, p64, p8, p4	pPL11::Tn*3*-spice derivatives (Fig. 2 and 4)	8b, 21

[a] Nal^r, Rif^r, Tet^r, Spc^r, Str^r, Amp^r, and Kan^r indicate resistance to nalidixic acid, rifamycin, tetracycline, spectinomycin, streptomycin, ampicillin, and kanamycin, respectively. Tn*3*-spice insertions outside functional *hrp* loci are designated *chr*::Tn*3*-spice.

involving ice nucleation assays, the growth temperatures were 24 to 25°C. M9 medium (26, 28) was used as the defined mineral salts medium for all strains. $MgSO_4$ was filter sterilized and added to the KB and M9 media after autoclaving. Similarly, carbon sources and antibiotics were added separately from concentrated filter-sterilized stocks at final concentrations of 0.2% for carbon sources, 15 μg/ml for tetracycline, 20 μg/ml for spectinomycin, streptomycin, and chloramphenicol, 50 μg/ml for nalidixic acid, and 100 μg/ml for rifamycin. β-Galactosidase indicator agar plates contained 25 μg of 5-bromo-4-chloro-3-indolyl-β-D-galactoside (Sigma Chemical Co.) per ml.

Molecular and genetic techniques. Enzyme reactions, plasmid transformations, and other routine molecular manipulations were carried out in *E. coli* HB101 or DH5α (highly competent cells; Bethesda Research Laboratories) as described previously (26). Stocks of recombinant plasmids were maintained in these *E. coli* hosts stored in glycerol or dimethyl sulfoxide at −80°C (26). Tn*3*-spice insertion derivatives were kept as described above in *E. coli* SF800 or HB101. Fresh cultures were prepared from these stocks before each experiment. Restriction endonucleases, other enzymes, and molecular biochemicals (from Bethesda Research Laboratories, Stratagene Inc., and Amersham Corp.) were used according to the recommendations of the supplier.

Plasmid minipreparations and total DNA were prepared as previously described (1, 3, 17). Extraction of intact native plasmids from strain NPS3121 was accomplished by the procedure of Kado and Liu (18). DNA was cross-linked to nylon membranes (Hybond N; Amersham) by UV irradiation and hybridized as described by Church and Gilbert (4). DNA probes were prepared by labeling with [α-^{32}P]dCTP (3,000 Ci/mmol; ICN Biomedicals, Inc.) and random oligonucleotide primers (Amersham). Plasmid transfers to *P. syringae* pv. phaseolicola were accomplished by triparental matings between the appropriate *E. coli* plasmid donor, the desired recipient, and *E. coli* HB101(pRK2013) as a conjugational helper strain (8). When strain NPS3121 or marker exchange mutants were used as recipients, optimal transfers were obtained with donor/recipient/helper ratios of 1:4:1 and 1:2:1, respectively.

Strains, libraries, and cosmids. *P. syringae* pv. phaseolicola NPS3121 was the parental strain of all mutants used in this study (Table 1). The cosmids and plasmid subclones originated from two genomic libraries of this strain, PspLib1 (35) and PspLib2 (8a, 33a). Both libraries consist of partially digested *Sau*3A fragments ligated into the *Bam*HI site of pLAFR3. The relevant properties of the strains and the plasmid constructs are given in Table 1 or described in detail below.

Cosmids pPL6 and pPL3 were isolated from PspLib1 as described previously (24), and pNN56 was isolated from

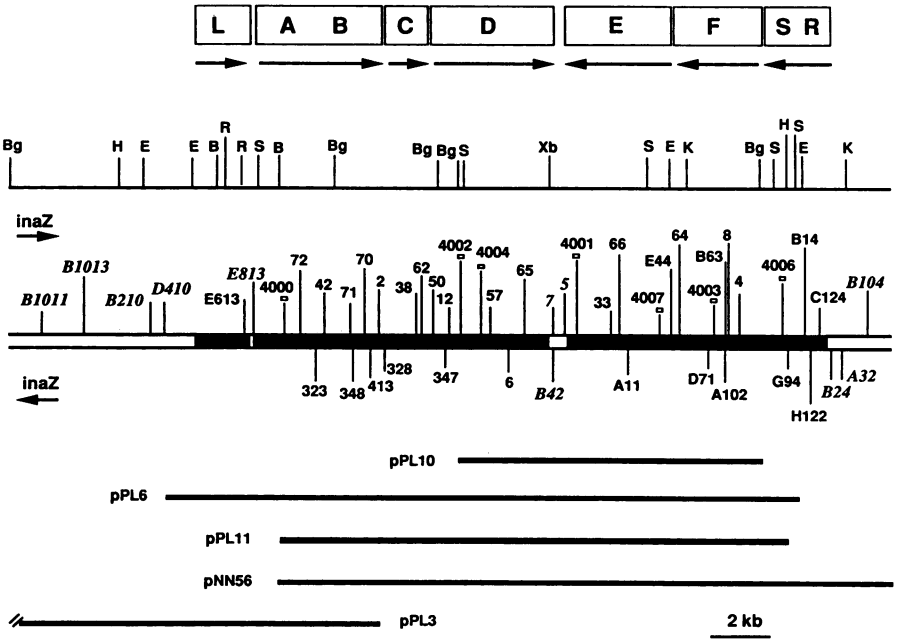

FIG. 1. *hrp* cluster of *P. syringae* pv. phaseolicola NPS3121. The open rectangles at the top and letters within them depict complementation groups as defined in the text, with the orientation of transcription indicated by the arrows. Endonuclease cleavage sites shown on the restriction map below the rectangles: H, *Hin*dIII; E, *Eco*RI; B, *Bam*HI; R, *Eco*RV (only the sites referred to in the text are shown); S, *Sac*I; Bg, *Bgl*II; Xb, *Xba*I; K, *Kpn*I. A map of the genomic insertions discussed in the text is shown below the restriction map, each with an identifying number as in Table 1 but without the NPS or LR prefixes. Tn*3*-spice insertions oriented from left to right and the insertions of the seven *hrp*::Tn*5* mutants are drawn above the line; Tn*3*-spice insertions oriented from right to left are drawn below the line. Insertions that produced Hrp$^+$ marker exchange haploids are shown in italics. Filled segments of the bar indicate functional *hrp* regions. The inserts of three cosmids and two subclones used in this work are shown in the lower part of the figure.

PspLib2 by colony probing with the 4.2-kb *Eco*RI-*Hin*dIII fragment from pPL6. These cosmids carried overlapping inserts that were colinear with the NPS3121 chromosome with respect to several restriction endonuclease cleavage sites and collectively covered the region between the outermost *hrp* mutations plus several kilobases further to the right and left (11a, 24; data not shown).

Plasmid constructions. The DNA fragments used to construct the various recombinant plasmids described below originated in plasmid pPL6 (Fig. 1) (24). Plasmid DNA was purified by dye-buoyant density gradient centrifugation and digested with the appropriate restriction endonucleases, and the fragments to be subcloned were separated by electrophoresis in low-melting-point agarose gels (Bio-Rad Corp.) and purified by phenol extraction.

(i) pLRBR, pLR32, and pLR86. The Tn*3*-spice derivative p7 (Table 1) of plasmid pPL11 (Fig. 1) was used as a source of a ca. 9.3-kb *Bam*HI-*Eco*RI fragment that was cloned between the synonymous sites of pLAFR3 to produce plasmid pLRBR (data not shown). Plasmid pLR32 is a pLAFR6 derivative carrying the 3.6-kb *Bgl*II fragment from pLRBR and was constructed in two steps. First, the 3.6-kb *Bgl*II fragment was cloned in the *Bam*HI site of plasmid BLUESCRIBE(+) (plasmid pLRB32; data not shown). Second, the insert was excised with *Eco*RI plus *Hin*dIII and cloned into the synonymous sites of pLAFR6. Plasmid pLR86 carries a 1.8-kb segment of the 3.6-kb *Bgl*II fragment excised from pLRB32 by digestion with *Pst*I (one site internal to the 3.6-kb insert and the other in the multilinker) and inserted upstream of the *inaZ* gene in pLAFR6-*inaZ*. The direction of *hrp* transcription across the 1.8-kb fragment (see Results) is the same as that of the *inaZ* gene. The choice of the pLAFR6-*inaZ* vector for the construction of pLR32 and pLR86 was not connected specifically to the use of these plasmids for complementation analysis but allowed them to be used in *hrp* gene regulation studies (36a).

(ii) pMM18. pMM18 carries the 2.1-kb *Bam*HI fragment derived from pPL6 inserted into the *Bam*HI site of plasmid pLAFR6-*inaZ*. The plasmid has the unique *Sac*I site of the insert located proximally to the native ATG codon of the *inaZ* gene (9, 22).

(iii) pMM3AS and pMM6AS. The 6.3-kb *Sac*I fragment from pPL6 was initially cloned into the *Sac*I site of pIBI76 to form plasmids pMMSA1 and pMMSA2 (data not shown). In these plasmids the unique *Bam*HI site of the *Sac*I insert was distal and proximal, respectively, to the *Bam*HI site of the pIBI76 polylinker. The insert was excised from pMMSA1 by digestion with *Eco*RI and *Hin*dIII, which cut the plasmid at unique sites in the vector polylinker, and was directionally cloned into pLAFR3 and pLAFR6 that had been digested with the same enzymes to produce plasmids pMM3AS and pMM6AS, respectively. The *lac* promoter of pLAFR3 drives the transcription of *hrp* sequences on the 6.3-kb *Sac*I fragment in pMM6AS in the orientation in which they are normally transcribed (see Results). In pMM6AS the pLAFR6 vector has no *lac* promoter, and the *hrp* sequences within the 1.8-kb insert are further insulated from vector promoters by the synthetic *trp* terminators flanking the pLAFR6 multilinker.

(iv) pMM6AS2. The 6.3-kb *Sac*I insert in pMM6AS was extended by cloning the 0.6-kb *Eco*RV-*Sac*I fragment into pMM6AS in two steps. First, the 0.6-kb *Eco*RV-*Bam*HI fragment was cloned into the vector pGEM7Zf(+); second, the insert was excised by digestion with *Eco*RI (multilinker

site) plus *Bam*HI and ligated to pMM6AS that had been digested with the same enzymes. The resulting plasmid, pMM6AS2, carries the 6.3-kb *Sac*I fragment and 0.6-kb *Eco*RV-*Sac*I fragment in their original relative positions and orientations.

Tn*3*-spice insertion mutagenesis of plasmids. The construction and properties of the Tn*3*-spice transposon have been described (22). The element is a modified Tn*3*-*lac* transposon (41) that carries a promoterless ice nucleation gene (*inaZ*) and permits the construction of transcriptional fusions but not translational fusions. The *inaZ* gene is located near the left terminus of the element and serves as a reporter of target gene transcription.

Tn*3*-spice insertion derivatives were constructed in this study by random mutagenesis of the plasmids pPL3 and pNN56 by the procedure of Stachel et al. (41) with the following modifications. First, *E. coli* SF800 was used as the host strain in place of strain C2110 because it yielded plasmid minipreparations of better quality. Second, *E. coli* HB101(pSShe, pTn*3*-spice) was mated with SF800 carrying the target plasmid by using HB101(pRK2013) as a conjugational helper strain. Transconjugants were selected on LB agar supplemented with tetracycline, spectinomycin, and nalidixic acid at 42°C, purified at the same temperature, and screened for sensitivity to chloramphenicol. The insertion points were mapped by single and/or double digestions of the mutant plasmids and by Southern blot hybridization as described below.

Construction of marker exchange haploids. Mutants carrying Tn*3*-spice insertions in the bacterial chromosome were obtained by marker exchange mutagenesis as follows: Tn*3*-spice derivatives of the plasmids pPL3, pNN56, and pPL11 were introduced into strain NPS3121 by triparental matings. The resulting merodiploids were grown in KB broth supplemented with rifamycin for five consecutive growth cycles (12 h each), followed by two to three cycles in the same medium supplemented with spectinomycin to allow for a double crossover and subsequent plasmid loss. The final cultures were serially diluted and plated on KB agar supplemented with spectinomycin. Presumptive marker exchange mutants were initially identified by replica screening for tetracycline sensitivity and spectinomycin and rifamycin resistance. Subsequently, these mutants were examined by Southern blot hybridization with appropriate segments of the *hrp* region as probes to verify their haploid genetic composition and the location of the Tn*3*-spice insertions.

Plant inoculations. Bean plants, cultivar Red Kidney (susceptible to infection by the wild-type strain), were used to establish the pathogenic phenotype of the mutant and merodiploid strains constructed in this study. The primary leaves of 8- to 12-day-old plants grown from seed in a greenhouse were inoculated by vacuum infiltration as described previously (24). For routine pathogenicity tests and quantitative studies of bacterial multiplication, bean leaves were inoculated with 5×10^5 CFU/cm^2 of leaf and 4×10^3 to 1.8×10^4 CFU/cm^2, respectively. Duplicate leaf disks (6-mm diameter, 0.28-cm^2 surface area) were removed at various times after inoculation and macerated in a total volume of 1 ml of sterile distilled water. Tenfold serial dilutions were prepared, and 0.1-ml aliquots were plated onto KB agar supplemented with spectinomycin and/or rifamycin to determine bacterial populations.

Tobacco plants, cultivar Turkish (which produce the hypersensitive response upon inoculation with the wild-type strain), were inoculated with 10^7 CFU/cm^2 of leaf to establish the nonhost-bacterium interaction phenotype of the above strains. A small incision was made in the interveinal leaf panels of 4- to 8-week-old plants, and inoculum suspensions were pressure infiltrated into the surrounding area with a sterile 1-ml plastic syringe. After inoculation, plants were kept in a growth chamber under an 18-h light, 6-h dark period at 20 to 25°C and 95% relative humidity until symptoms appeared in the control plants inoculated with the wild-type strain (overnight for tobacco inoculations and 4 to 6 days for bean inoculations).

Gene expression assays. The level of expression of *hrp*::*inaZ* fusions was quantified by means of droplet freezing assays as described by Lindgren et al. (22). In vitro expression levels were determined for cultures grown in KB broth as well as in planta at 24 to 25°C by using cells grown in KB broth as a starter inoculum. Approximately 3×10^4 CFU/cm^2 were administered to leaves by vacuum infiltration. Duplicate leaf disks were removed immediately after and at 24 h after inoculation. After tissue maceration and serial dilution, the ice nucleation activity was assayed at −9°C. The same serially diluted aliquots were used to determine bacterial populations by plating onto KB agar supplemented with rifamycin and tetracycline. The ice nucleation activity was expressed as the negative logarithm of the number of ice nuclei per CFU (INA units).

RESULTS

The *hrp* cluster spans 22 kb, is genetically contiguous, and is chromosomally located. Of the eight *hrp*::Tn*5* mutants isolated by Lindgren et al. (24), seven (NPS4000, NPS4002, NPS4004, NPS4001, NPS4007, NPS4003, and NPS4006) had the transposon inserted within a 17.5-kb segment of the *P. syringae* pv. phaseolicola NPS3121 genome, indicating that a number of genes associated with *hrp* functions were present in the regions surrounding these mutations (Fig. 1). The focus of the present study was initially to saturate the regions around these mutations with transposon insertions and to analyze the mutants for their ability to cause disease symptoms on Red Kidney beans and to elicit the hypersensitive reaction on tobacco. After this analysis, detailed investigation of the genetic organization of this region, the direction of *hrp* gene transcription, and level of expression in planta was carried out, and the effect of mutations in each locus on the ability of the bacterium to multiply in bean leaves was examined.

Two cosmid clones, pPL3 and pNN56 (Fig. 1), were selected for insertional mutagenesis based upon their ability to span the above region plus several kilobases to the right and left of the outermost mutations previously described (NPS4000 and NPS4006). Each cosmid was mutagenized with the reporter transposon Tn*3*-spice, and several hundred insertions were generated. The precise location of each insertion was determined by multiple restriction enzyme mapping. A similar set of mutations in the plasmid pPL11 that had been previously mapped (22) was also employed in the present study. Selected insertions in these three plasmids that were spaced from 0.1 to 1 kb apart and represented both orientations were chosen for the construction of marker exchange haploids in the wild-type strain NPS3121 (Fig. 1). A total of 43 haploids were generated (Fig. 1) and verified by Southern hybridization analysis with respect to their haploid structure and position of the mutations (data not shown).

Thirty of the marker exchange mutants were phenotypically Hrp$^-$, i.e., unable to produce watersoaked lesions on Red Kidney bean leaves and to elicit the hypersensitive response on tobacco. Two mutants, LR38 and LR62, also

TABLE 2. Complementation analysis of the *hrp* cluster of *P. syringae* pv. phaseolicola

Group	Genomic mutant(s)	Complementing plasmids	Noncomplementing plasmids
hrpL	LRE613	pPL6 (Fig. 2)	pMM18 (Fig. 2)
hrpAB	NPS4000	pE613, pE813 (Fig. 2)	pPL1
	LR72, LR70, LR2	(Fig. 2)	pPL1
	LR72, LR323, LR42, LR71, LR348, LR70, LR413, LR2, LR328	(Fig. 2)	(Fig. 2)
hrpC	LR38, LR62	pPL1, p328, p50, p12, p57 (Fig. 2)	p38, p62 (Fig. 2)
hrpE	NPS4001	pB53, pH84	pC52, p66, pA11, pF94
	LR66	pH84	pC52, pA11
	LRA11		pF94
	NPS4007	p7, p64, pH84, pPL10	p66, pA11
	LRE44	p64, pH84, pA102, pB63	pC52, p66, pA11, pE44
hrpF	LR64	pH48, pF94, pE44, pB24, pPL10	p64, pA34, pD71, pA102, pB63
	LRD71	pC52, p66, pA11, pPL10	p64, pA34
	LRB63	pPL10, pB14	p64
	LR8	p66, pH102	p64, pD71, pA102, pB63
	LR4	pG94, pC124	pD71, pB63
hrpSR	NPS4006	pD71, pH84, pB63, pA32, pB102	pG94, pH122, pH124
	LRG94	pA102, pNN56	pG94
	LRH122	pD71, pB63	pB114, pC124, pPL10
	LRC124	pH84, pB63, pA21, pB104, pNN56	pG94, pB14, pH94

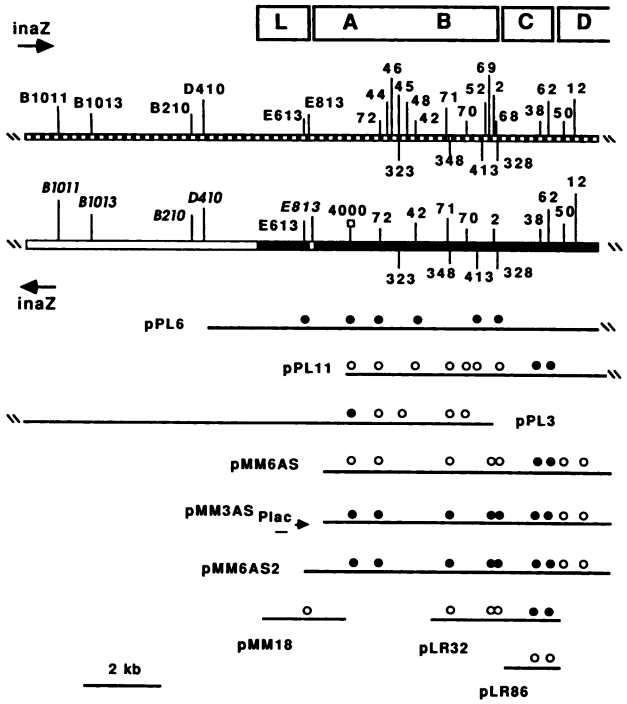

FIG. 2. Complementation analysis of the region composed of *hrpL*, *hrpAB*, and *hrpC*. Open rectangles at the top depict the assignments of complementation groups. Tn*3*-spice insertions on plasmids (top line), genomic insertions (second line), and plasmids (several lines below) were employed in complementation analysis of *hrpL*, *hrpAB*, and *hrpC*. Insertions are depicted and identified as in Fig. 1. Filled and open circles above each plasmid indicate complementation and lack of complementation, respectively, of the genomic mutation corresponding to the position of the dots. The P*lac* promoter on the left side of the pMM3AS insert is that of the pLAFR3 vector. Other details are as in Fig. 1.

failed to elicit the hypersensitive response on tobacco but gave attenuated disease symptoms (as described below). All 32 mutants were restored to the wild-type phenotype by at least one of the cosmids and/or by plasmids carrying the appropriate subcloned fragments (Table 2; Fig. 2 and 4). Therefore, the Hrp$^-$ phenotype of the marker exchange mutants was attributed to the Tn*3*-spice insertions within the complemented region.

Eleven marker exchange mutants (Fig. 1) produced normal water-soaked lesions on Red Kidney beans and elicited typical hypersensitive necrosis on tobacco. The mutations were located as follows: LRB1011, LRB1013, LRB210, and LRD410 were within a 7-kb region segment to the left of the LRE613 insertion, the leftmost mutation that produced a Hrp$^-$ marker exchange haploid; LRE813 defined an intergenic region just to the right of the leftmost *hrp* locus, *hrpL*; LRB42, LR5, and LR7 lay between the *hrpD* and *hrpE* complementation groups (see below); and LRB24, LRA32, and LRB104 were located within 1.5 kb to the right of insertion LRC124, the rightmost mutation that produced a marker exchange haploid. Based on these results and on the complementation data discussed below, we conclude that

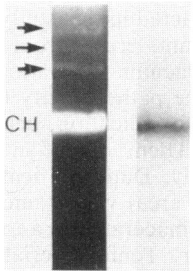

FIG. 3. Southern blot of DNA extracted from strain NPS3121 by the method of Kado and Liu (18). The same gel is shown after ethidium bromide staining (left) and after hybridization with [^{32}P]dCTP-labelled pPL11 plasmid DNA (right). The hybridization signal is insert specific. Arrows on the left mark the location of plasmid bands that were visible with ethidium bromide staining. The more prominent fastest moving band (CH) is chromosomal DNA.

the *hrp* cluster of strain NPS3121 is essentially contiguous and spans nearly 22 kb.

To establish the position of the *hrp* cluster in the genomic elements of *P. syringae* pv. phaseolicola, a procedure that yields intact plasmid molecules that can be separated from chromosomal DNA was applied (18). Four plasmid bands migrating slower than the chromosomal DNA were detected by ethidium bromide staining, indicating the presence of large plasmids in the wild-type strain NPS3121 (Fig. 3). A Southern blot of this gel hybridized with ^{32}P-labeled *hrp* DNA (plasmid pPL11) gave a distinct signal only in the position where the chromosomal DNA had migrated (Fig. 3), indicating that the *hrp* cluster is chromosomally located in this strain.

Genetic organization of the *hrp* region. To genetically define the functional units within the *hrp* cluster, complementation analysis of the available genomic mutants was carried out. Tn*3*-spice insertion derivatives of cosmids pPL3, pNN56, and pPL11, as well as plasmids carrying subcloned *hrp* DNA inserts, were introduced into the genomic mutants, and the phenotypes of the resulting merodiploids were determined by inoculation onto both Red Kidney beans and tobacco leaves. Selected plasmid-mutant combinations were used, based on the results obtained during the course of the investigation. Since the DNA insert in plasmid pPL11 lacks the promoter region necessary for complementation of many chromosomal mutants with insertions in the *hrpAB* region (see below), the complementation strategy followed for the left part of the *hrp* cluster relied chiefly on plasmids carrying subcloned *hrp* inserts. Each functionally distinct region is discussed separately below starting from the left (Fig. 1 and 2).

(i) *hrpL*. The insertion in LRE613 is the leftmost mutation that produced an Hrp$^-$ marker exchange haploid strain and was mapped near the middle of the 2.1-kb *Bam*HI fragment (Fig. 1). Plasmid pPL6, which has an insert that extends about 2 kb to the left, complemented LRE613, but plasmid pMM18, which carries the 2.1-kb *Bam*HI insert, failed to do so (Fig. 2). Therefore, the leftmost *hrp* locus in the *hrp* cluster, designated *hrpL*, apparently extends 1 to 1.8 kb to the left of the LRE613 mutation and has its right border within 0.1 kb of the LRE813 insertion.

(ii) *hrpAB*. The complementation pattern obtained with nine marker exchange mutants with insertions located to the right of LRE813 (NPS4000, LR72, LR323, LR42, LR348, LR70, LR413, LR2, and LR328) and with the plasmids depicted in Fig. 2 allowed us to define two functionally linked loci immediately to the right of *hrpL*. These nine mutants were distinguished from those carrying insertions further to the right in that they were not complemented by pPL11. All nine mutants were complemented by plasmids pMM6AS2, pMM3AS, and pPL6 but not by pMM6AS. The last plasmid lacks the 0.6-kb *Eco*RV-*Sac*I segment present on the left side of the pMM6AS2 insert, whereas pMM3AS differs from pMM6AS in that only the former has the vector *lac* promoter, which provides rightward transcription into the 6.3-kb *Sac*I insert. Based on our *inaZ* expression analysis (see below), the direction of transcription in this region is from left to right. Therefore, the 0.6-kb *Eco*RV-*Sac*I fragment in pMM6AS2 must contain a promoter, and the 6.3-kb *Sac*I fragment has an intact coding region corresponding to the group of mutations discussed above.

One of the nine genomic mutants described above (NPS4000) was unique in that it was the only one in the group that could be complemented by plasmid pPL3 (Fig. 2). Neither this nor three other mutants from this group were

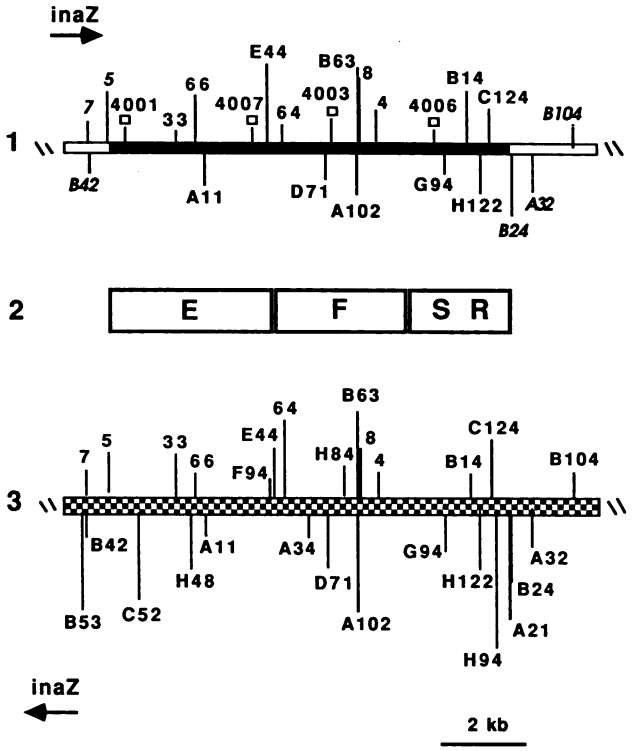

FIG. 4. Complementation analysis of the region composed of *hrpE*, *hrpF*, and *hrpRS*. Genomic mutations (top line) and Tn*3*-spice insertions on plasmids (bottom line) are depicted according to the Fig. 1 and 2 legends. The complementation groups deduced are shown as rectangles in the middle of the figure.

complemented by plasmid pPL1 (Table 2). The pPL1 insert covers this region, and pPL1 complemented mutations in an adjacent locus further to the right (*hrpC*; see below). This plasmid carries the Tn*5* insertion present in NPS4000 (23). This mutation apparently has a polar effect on the region located to its right, based on the results obtained with pPL1, pMM6AS, pMM3AS, and pMM6AS2 (Fig. 2 and Table 2). Evidently, pPL3 does not contain the entire functional unit in which this group of mutants belongs. Accordingly, we propose that two functional units, designated *hrpAB*, are located in the region starting just to the right of the LRE813 insertion and including the insertion in LR328.

(iii) *hrpC*. *hrpC* was defined on the basis of the complementation of two mutants, LR38 and LR62, by the plasmids depicted in Fig. 2 as well as with pPL11::spice derivatives (Table 2). All plasmids tested except p38, p62, and pLR86 complemented both mutants to the wild-type phenotype (Fig. 2). The pLR86 insert corresponds to the rightmost 1.8-kb *Pst*I-*Bgl*II segment of the 3.6-kb insert of pLR32 and extends just to the right of the LR328 insertion, which belongs to the *hrpAB* complementation group. Accordingly, a functionally distinct locus, here designated *hrpC*, lies between the *hrpAB* and *hrpD* loci. Assuming that pLR86 does not contain a functional *hrpC* promoter, we propose that the left and right borders of this locus lie between the LR328 and LR50 mutations.

(iv) *hrpD*. *hrpD* has been genetically analyzed by Lindgren et al. (22) and Frederick (8a). Mutants LR6 and LR65 constructed in this study were phenotypically Hrp$^-$ and were not complemented by plasmid p12. This, taken together with the results of the other two studies above,

indicates that this locus, designated *hrpD*, includes the insertions from LR50 to LR65. DNA sequence analysis places the right border of the *hrpD* coding region 80 bp to the left of the unique *Xba*I site (8a).

(v) ***hrpE.*** *hrpE* was defined as a distinct genetic group based upon the complementation analysis of five mutants, NPS4001, LR66, LRA11, LR4007, and LRE44, by a set of pNN56::Tn*3*-spice insertion derivatives and by plasmid pPL10 (Fig. 1 and 4, Table 2). Plasmids pC52, pH48, p66, pA11, pF94, and pE44 did not complement any of these five mutants, whereas pPL10 complemented all five. Furthermore, Tn*3*-spice insertions in pNN56 that were located to the right of LRE44 complemented this group of mutants. We conclude that the region defined by the above mutations constitutes a single complementation group, designated *hrpE*, which extends from the left of mutation NPS4001 to the right of mutation LRE44.

(vi) ***hrpF.*** Five marker exchange mutants with insertions located within the 3-kb *Eco*RI-*Bgl*II segment (LR64, LRD71, LRB63, LR8, LR4) and five Tn*3*-spice insertion plasmids (p64, pA34, pD71, pB63, pA102) did not cross-complement. However, four of these mutants were complemented by plasmids with insertions located outside this segment and by pPL10 (Table 2, Fig. 4). Based on these results, we define the *hrpF* locus as the region starting immediately to the right of *hrpE* and extending to the right between the LR4 mutation and the *Bgl*II site, which overlaps the putative termination codon of *hrpS* (10) (see below).

(vii) ***hrpSR.*** Grimm and Panopoulos (11) previously described a gene (*hrpS*) with a coding region within the 1.1-kb *Hin*dIII-*Bgl*II fragment (Fig. 1). This gene encodes a 35-kDa protein that resembles the activator domain of the nitrogen regulator protein NtrC and other similar proteins (11, 12). Four Hrp$^-$ mutants isolated in this study (LRG94, LRB14, LRH122, and LRC124) had insertions in the vicinity of NPS4006 as well as further to the right, where no Hrp$^-$ mutations were previously reported (Fig. 1 and 4). The mutation in LRG94 was located within the 1.1-kb *Bgl*II-*Hin*dIII fragment, whereas those in LRB14, LRH122, and LRC124 were located within 1 kb to the right of *Hin*dIII. The above five mutants did not cross-complement with plasmids pG94, pH122, pB14, pH94, and pC124. Furthermore, plasmids pD71, pH84, pB63, pA32, and pB104 complemented the four mutants in this group with which they were tested (Table 2). Keeping the previous genetic assignment for *hrpS*, we designate the region corresponding to the complementation group identified above as *hrpSR*. This is the rightmost locus of the *hrp* cluster identified in our study and extends from the *Bgl*II site, which overlaps the putative *hrpS* termination codon (11), rightward to the pA21 insertion (Fig. 4).

Transcriptional orientation and expression of *hrp* genes in Red Kidney bean leaves. To establish the orientation in which the *hrp* loci are described, we exploited the reporter gene function of the promoterless *inaZ* gene under conditions previously shown to promote expression of the *hrpD* locus, namely, inoculation onto bean leaves (22). In the course of this study, it became apparent that NPS3121 merodiploid strains carrying Tn*3*-spice insertions on plasmids express higher levels of ice nucleation activity when compared with those of merodiploids carrying the same insertions in the chromosome [e.g., the log INA units for NPS3121(p12) and LR12(pLRBR) grown in KB broth were −3.7 and −7.5, respectively]. This is a general feature of the *inaZ* reporter, which is particularly sensitive to perturbations caused by vector promoters and plasmid copy number due to the nonlinear relationship between the amount of ice nucleation protein and the signal it generates (22, 40). Accordingly, the direction of *hrp* gene transcription (Fig. 1 and 5) was deduced from measurements of ice nucleation activity of complemented merodiploids carrying the *inaZ* reporter in the chromosome. These measurements were made in the inoculum as well as in bean leaves at 0 and 24 h postinoculation.

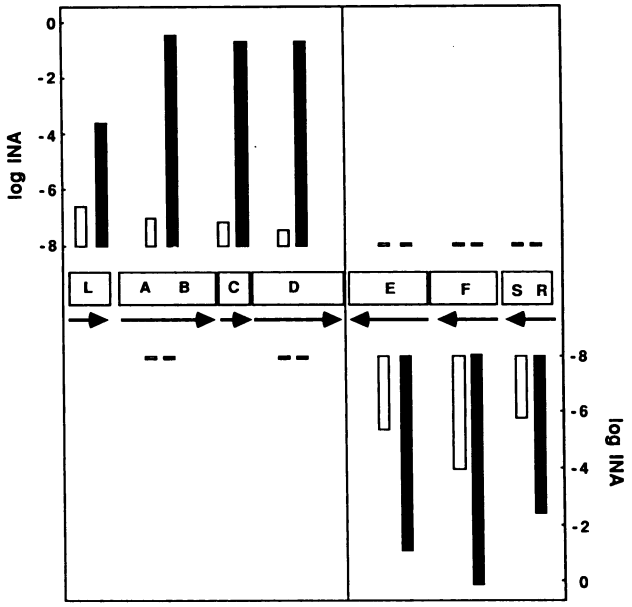

FIG. 5. Schematic illustration of basal and induced *inaZ* expression levels in complemented merodiploids carrying chromosomal *hrp*::*inaZ* fusions (Table 3) in the two possible orientations and in each complementation group. Bar heights are based on one or two insertions (averaged) as shown in Table 3. Symbols: □, ice nucleation activity levels measured in the KB broth just before inoculation (chosen as more representative of the initial expression levels in planta for reasons described in the text); ■, activities measured in bean leaves at 24 h postinoculation. The upper panel shows activities of strains with the *inaZ* gene oriented from left to right; the lower panel shows activities of strains with *inaZ* oriented from right to left. Rectangles in the middle depict the complementation groups as in the previous figures.

Ice nucleation activities were either undetectable or extremely low in bean leaves immediately after inoculation. This was expected, because the number of bacterial cells deposited initially in a leaf area equal to the size of a sample (0.56 cm^2) is about 1.5×10^4 CFU, which is too low for detection or accurate quantification of ice nucleation activity in most uninduced cultures. More concentrated inocula were purposefully avoided because they elicit normosensitive necrosis (21). Therefore, the activities determined in the KB broth-grown inoculum just before infiltration were used as uninduced reference values.

Strains with the *inaZ* gene fused in a rightward orientation in *hrpL*, *hrpAB*, and *hrpC* and in a leftward orientation in *hrpE*, *hrpF*, and *hrpSR* expressed significantly higher ice nucleation activities in bean leaves at 24 h postinoculation compared with their corresponding activities in KB broth, as previously established for *hrpD* (22). The deduced orientation of transcription in each locus is shown in Table 3 and Fig. 1 and 5. Although no mutations with the *inaZ* gene oriented from right to left were available in *hrpL* and in *hrpC*, the behavior of oppositely oriented insertions in the other four loci supports our conclusion concerning the

TABLE 3. Expression levels of chromosomal *hrp*::*inaZ* fusions in merodiploids

Locus	Strain	Log INA units[a]		Fold induction[b]
		KB medium	Bean leaves	
hrpL	LRE613(pPL6)	−5.60	−3.70	9
hrpAB	LR72(pMM6AS2)	−6.90	−0.01	2,313
	LR70(pMM6AS2)	−6.80	−0.27	
	LR328(pMM6AS2)	<−8.00	<−8.00	
	LR323(pMM6AS2)	<−8.00	<−8.00	
hrpC	LR38(pLRBR)	−7.50	−0.97	1,626
	LR62(pLRBR)	−6.90	−0.60	
hrpD	LR50(pLRBR)	−7.50	−0.40	2,726
	LR12(pLRBR)	−7.50	−0.95	
	LR347(pLRBR)	<−8.00	<−8.00	
hrpE	LRA11(pPL10)	−5.30	−1.08	129
	LR66(pPL10)	<−8.00	<−8.00	
	LRE44(pPL10)	<−8.00	<−8.00	
hrpF	LRD71(pPL10)	−4.00	0.06	105
	LRA102(pPL10)	−4.00	0.03	
	LR64(pPL10)	<−8.00	<−8.00	
	LRB63(pPL10)	<−8.00	<−8.00	
hrpSR	LRG94(pNN56)	−5.90	−2.50	50
	LRH122(pNN56)	−6.00	−2.50	
	LRC124(pNN56)	<−8.00	<−8.00	
	LRB14(pNN56)	<−8.00	<−8.00	

[a] Units are the number of ice nuclei per cell, calculated as described in the text and expressed here by their negative logarithms. Activity below 10^8 INA units was nondetectable. Values for each mutant are averages of duplicate determinations, each carried out in a two-leaf disk sample (0.56-cm^2 total leaf area). Ice nucleation activities within each pair of samples differed from each other two- to fourfold (0.3 to 0.6 log INA units).

[b] Induction ratios were calculated as the square root of the difference between ice nucleation activities determined for the particular strain in KB broth and in bean leaves. When two inducible insertions in the same locus were used, induction ratios were calculated from the average difference of both insertions. For other details, see the text.

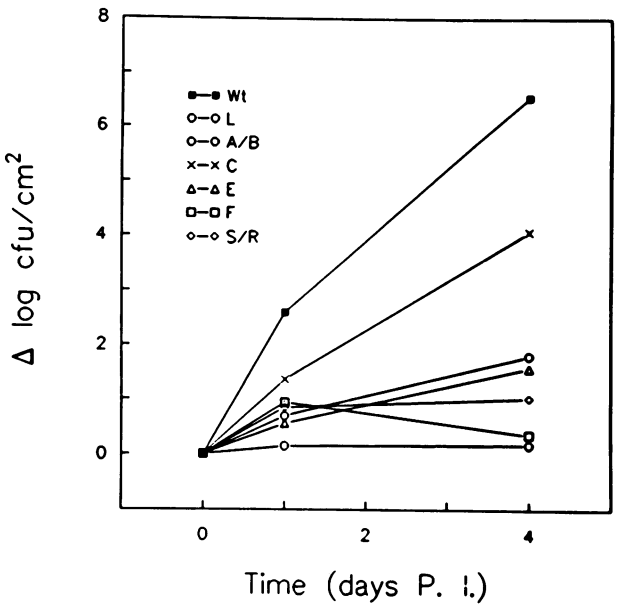

FIG. 6. Time course of multiplication of *hrp* mutants in Red Kidney bean leaves. Data are averages of duplicate samples taken at each sampling point, each sample consisting of two leaf disks (0.56-cm^2 total leaf area). The values for the duplicate samples differed from each other less than threefold. Mutants in each complementation group had essentially identical growth curves; therefore, the data for mutants within each locus were averaged, except for the sole *hrpL* mutant (LRE613). Insert legend: Wt, NPS3121; L, LRE613; A/B, average of LR72 and LR70; C, average of LR38 and LR62; E, average of LRA11 and LRE44; F, average of LRD71 and LRA102; S/R, average of LRG94 and LRC124 (the lowest line applies to A/B).

orientation of transcription in *hrpL* and *hrpC*. The expression levels obtained with two different insertions in each locus and each orientation were essentially identical (Table 3). Therefore, the results reflect the properties of the loci themselves rather than of the specific fusion.

The degree of induction for each locus was calculated from the ratio of activities in bean leaves to those in KB medium based upon the square power relationship between the amount of InaZ protein and the ice nucleation activity deduced in previous studies (22). The values obtained (Table 3) varied from 9-fold for *hrpL* to over 1,000-fold for *hrpAB*, *hrpC*, and *hrpD*. In the case of *hrpAB*, *hrpD*, *hrpC*, and *hrpF* the true values are probably underestimated, because the activity levels in bean leaves approached or exceeded 0.4 INA units ($\log_{10}$ INA, −0.6), where the square power relationship does not strictly apply (40). The *hrpL* and *hrpSR* loci showed low expression levels in bean leaves and low degrees of induction. All other loci showed high expression levels in bean leaves as well as high degrees of induction but with considerable variation among them. The differences in the degree of induction of *hrpE* and *hrpF* compared with those of *hrpAB*, *hrpC*, and *hrpD* reflected largely the differences in their respective basal expression levels.

Multiplication of *hrp* mutants in Red Kidney bean leaves. In previous studies (24), the ability of *hrp*::Tn*5* mutants of *P. syringae* pv. phaseolicola to multiply in Red Kidney bean leaves was greatly reduced (10^5-fold) compared with that of the wild-type strain, except for NPS4003, whose growth was reduced only about 10-fold. In the present study, the growth of two or more mutants from each complementation group (except *hrpL*, for which only one mutant was available) was determined in Red Kidney bean leaves. Mutants with insertions in *hrpL*, *hrpAB*, *hrpD*, *hrpE*, *hrpSR*, and in *hrpF*, where NPS4003 is also located, reached roughly 10^5- to 10^7-fold-lower population levels than did the wild-type strain at 4 days after inoculation (Fig. 6). However, the *hrpC* mutants reached population levels only 10^2-fold lower than those of the wild-type strain and still produced water-soaked lesions in this cultivar. However, these lesions were delayed by several days and were both smaller in size and fewer in number than those of the wild-type strain. Colonies isolated from single lesions retained the genetic characteristics of the original mutants and gave identical symptoms when inoculated on Red Kidney bean leaves. The above results rule out the possibility that the lesions were produced by genetic revertants and suggest that *hrpC* functions differently from other *hrp* loci in the bacterium-plant interaction.

DISCUSSION

The present study establishes the genetic and transcriptional organization of the *hrp* cluster from *P. syringae* pv. phaseolicola and clarifies several other questions about *hrp* gene expression that had not been adequately addressed by previous investigations. The cluster comprises seven complementation groups, designated *hrpL*, *hrpAB*, *hrpC*, *hrpD*, *hrpF*, *hrpE*, and *hrpSR*, and encodes functions involved in the plant-bacterial interaction essentially throughout its length. A short region near the approximate middle of the cluster does not appear to control the interaction between

the bacterium and the two indicator plants used in this study. The functional length of the cluster is about 22 kb, which is similar to the size of the synonymous cluster of the related pathogen *P. syringae* pv. glycinea deduced from Tn*5* mutagenesis (16). The *hrp* cluster of *P. syringae* pv. syringae appears to be roughly similar in size (45a). The cluster is located on the chromosome of strain NPS3121. Although we did not examine other strains of the pathogen in this regard, it is interesting to note that an *hrp* cluster of similar size described in *P. solanacearum* is located on a megaplasmid (2). This is also the case with other large gene groups that control the plant-bacterium interactions in crown gall disease and in *Rhizobium*-legume symbiosis.

Several of the complementation groups identified in this study occupy rather large regions, suggesting that each of these loci encodes either a very large polypeptide or several polypeptides (preliminary data suggest the latter for *hrpF* and *hrpD* [10a]). Other work (11, 11b) has established that the *hrpSR* locus encodes two proteins that show sequence similarity with each other as well as with several NtrC-like proteins. Another noticeable feature of the *hrp* cluster is its transcriptionally convergent organization; the genes located in its left portion are transcribed from left to right, whereas those located in its right portion are transcribed in the opposite direction. The significance of this arrangement is not immediately apparent.

The *inaZ* fusion system used in our studies is clearly superior to conventional reporter systems for bacterial gene expression studies carried out in planta. The expression levels recorded in KB broth are in fact quite low and would not be detectable by conventional reporters. Such reporters could detect the in planta expression of *hrp* genes only when high inoculum concentrations were employed (which could produce artifacts [20]) or when the bacteria had opportunity to multiply in the plant tissue, such as on susceptible hosts at later stages of infection (compatible interactions). However, as further discussed below and elaborated in more detail elsewhere (22, 40), the *inaZ* reporter also has certain peculiarities that we took into consideration in designing our approach to the transcriptional studies. For example, because of its high sensitivity and the nonlinear relationship between the amount of InaZ protein and the signal produced, the system amplifies vector promoter effects upon cloned genes and is sensitive to gene dosage (vector copy number). The use of strains carrying chromosomal *hrp*::*inaZ* fusions eliminated the above factors as potential sources of "noise" in the present study.

The quantitative interpretation of ice nucleation activity data in terms of target gene transcription has been extensively discussed elsewhere (22, 40). Three significant points may be mentioned here to place the quantitative analysis of *hrp* gene expression data in proper perspective. Ice nucleation activities determined in whole-cell suspensions approach asymptotically a theoretical maximum of 1 INA unit ($\log_{10}$ INA, 0). When the assays are carried out at −9°C, the quantitative relationship between the amount of InaZ protein and the signal it generates is a square power function over a large range of activities and protein concentrations. This relationship holds up to about 0.4 INA units ($\log_{10}$ INA, 0.6), where it changes to a more linear relationship.

In light of this information, we consider our ice nucleation activity data from a quantitative standpoint. First, within each complementation group fusions in only one orientation showed significant activity, either in KB broth or in bean leaves. Furthermore, only these fusions gave higher ice nucleation activities in bean leaves relative to those in KB broth, by several $\log_{10}$ units in each case. These results clearly establish the direction of transcription for all seven *hrp* complementation groups. Second, the maximum ice nucleation activities obtained for some *hrp*::*inaZ* fusions (e.g., those in *hrpAB*, *hrpC*, *hrpD*, and *hrpF*) were in the linear dose-response range for the *inaZ* reporter and approached the theoretical maximum of 1 INA unit. Therefore, it is not certain that the activities measured in these cases reflect equal levels of transcription of the target genes under induced conditions. Nevertheless, the ice nucleation activities recorded with these *inaZ* fusions plus those in *hrpE* in bean leaves were considerably greater than the activities recorded with fusions to *hrpL* and *hrpSR*. Finally, the degree of induction, calculated from the ratio of activities in bean leaves to those in KB medium, were considerably lower from *hrpL* and *hrpSR* compared with those for the other loci. This implies fundamentally different regulatory mechanisms for *hrpL* and *hrpSR* compared with those for the other genes. As reported elsewhere (10, 11, 30, 36), the *hrpS* gene is a positive regulator of *hrpAB*, *hrpC*, and *hrpD* expression. Regulatory functions have also been proposed for genes located at the termini of the *hrp* cluster of *P. syringae* pv. glycinea (16), where *hrpL* and *hrpSR* homologs presumably reside.

As noted previously by us and other authors (2, 5, 7, 14, 24, 25, 37, 39, 44, 45), *hrp* mutants of bacteria are prototrophic and have invariably reduced ability to multiply in susceptible host tissues. The present study showed that both of these features apply to all *hrp* loci identified by our complementation analysis. However, *hrpC* differed from the other *hrp* loci in that the two *hrpC* mutants, although unable to elicit hypersensitive necrosis on tobacco, produced attenuated symptoms on Red Kidney beans. Such symptoms were previously obtained with one *hrpF*::Tn*5* mutant (24) but not with any other *hrpF* mutants generated in this study. Therefore, the attenuated phenotype of the above mutant most likely reflects the specific insertion (promoter generation?) rather than the properties of the *hrpF* locus. The basis of the attenuated phenotype of *hrpC hrpF* mutants and the role of these loci in the plant-bacterium interaction are currently under investigation.

The function of most *hrp* genes in the plant-bacterium interaction remains unknown. Knowledge of the overall structure and organization of the *hrp* cluster has greatly assisted our investigations into *trans*-acting factors and physiological mechanisms that regulate the expression of *hrp* genes in planta and in vitro (11, 30, 36a). Some *hrp* genes are expressed in vitro but only under certain conditions (30, 47). The possible involvement of specific plant signals in *hrp* gene expression in planta has not been ruled out and is currently under investigation. Our study provides an experimental foundation to guide further structural, functional, and regulatory analyses of the region toward the ultimate understanding of the molecular mechanisms by which *hrp* genes control the bacterium-plant interaction.

ACKNOWLEDGMENTS

This work was supported by grant DMB-8706129 from the National Science Foundation and by the California Biotechnology Program.

We thank Barbara Lastelic and Annamaria Pisi for technical assistance, S. E. Lindow for routine use of his facilities for ice nucleation assays, B. J. Staskawicz and D. Dahlbeck for providing pLAFR6 and sharing information and data with us before publication, R. D. Frederick for use of PSP-Lib2, and R. D. Frederick and Aria A. Tzika for constructive suggestions during preparation of the manuscript.

REFERENCES

1. **Birnboim, H. C., and J. Doly.** 1979. A rapid alkaline extraction procedure for screening recombinant plasmids. Nucleic Acids Res. **7**:1513–1523.
2. **Boucher, C. A., F. Van Gijsegem, P. A. Barberis, M. Arlat, and C. Zischek.** 1987. *Pseudomonas solanacearum* genes controlling both pathogenicity on tomato and hypersensitivity on tobacco are clustered. J. Bacteriol. **169**:5626–5632.
3. **Chesney, R. H., J. Rothman Scott, and K. Vapnek.** 1979. Integration of the plasmid prophages p1 and p7 into the chromosome of *Escherichia coli*. J. Biol. Chem. **130**:161–173.
4. **Church, G. M., and W. Gilbert.** 1984. Genomic sequencing. Proc. Natl. Acad. Sci. USA **81**:1991–1995.
5. **Cuppels, D. A.** 1986. Generation and characterization of Tn*5* insertion mutations in *Pseudomonas syringae* pv. *tomato*. Appl. Environ. Microbiol. **51**:323–327.
6. **Daniels, M. J., J. M. Dow, and A. E. Osburn.** 1988. Molecular genetics of pathogenicity in phytopathogenic bacteria. Annu. Rev. Phytopathol. **26**:285–312.
7. **Deasey, M. C., and A. C. Matthysse.** 1988. Characterization, growth and scanning electron microscopy of *Pseudomonas syringae* pv. *phaseolicola* mutants which fail to elicit a hypersensitive response in host and non-host plants. Physiol. Mol. Plant Pathol. **33**:443–457.
8. **Ditta, G., S. Stanfield, D. Corbin, and D. R. Helinski.** 1980. Broad host range DNA cloning system for Gram-negative bacteria: construction of a gene bank of *Rhizobium meliloti*. Proc. Natl. Acad. Sci. USA **27**:7347–7351.

8a. **Frederick, R. D.** 1990. Ph.D. thesis. University of California, Berkeley.

8b. **Frederick, R. D.** Unpublished data.

8c. **Frederick, R. D., and N. J. Panopoulos.** Unpublished data.

9. **Green, L. R., and G. J. Warren.** 1985. Physical and functional repetition in a bacterial ice nucleation gene. Nature (London) **317**:645–648.
10. **Grimm, C., L. Rahme, R. D. Frederick, M. Mindrinos, P. Lindgren, and N. J. Panopoulos.** 1989. The common pathogenicity genes of *Pseudomonas syringae* pathovars. UCLA Symp. Mol. Cell. Biol. **101**:49–55.

10a. **Grimm, C. G., R. D. Frederick, and N. J. Panopoulos.** Unpublished data.

11. **Grimm, C. G., and N. J. Panopoulos.** 1989. The predicted protein product of a pathogenicity locus from *Pseudomonas syringae* pv. *phaseolicola* is homologous to a highly conserved domain of several procaryotic regulatory proteins. J. Bacteriol. **171**:5031–5038.

11a. **Grimm, C. G., and N. J. Panopoulos.** Unpublished data.

11b. **Grimm, C. G., N. J. Panopoulos, B. J. Staskawicz, and D. Dahlbeck.** Unpublished data.

12. **Gross, R., B. Arico, and R. Rappuoli.** 1989. Families of bacterial signal-transducing proteins. Mol. Microbiol. **3**:1661–1667.
13. **Huang, H.-C., R. Schuurink, T. P. Denny, M. M. Atkinson, C. J. Baker, I. Yucel, S. W. Hutcheson, and A. Collmer.** 1988. Molecular cloning of a *Pseudomonas syringae* pv. *syringae* gene cluster that enables *Pseudomonas fluorescens* to elicit the hypersensitive response in tobacco plants. J. Bacteriol. **170**: 4748–4756.
14. **Huang, Y., P. Xu, and L. Sequeira.** 1990. A second cluster of genes that specify pathogenicity and host response in *Pseudomonas solanacearum*. Mol. Plant-Microbe Interact. **3**:48–53.
15. **Hutcheson, S. W., A. Collmer, and J. C. Baker.** 1989. Elicitation of the hypersensitive response by *Pseudomonas syringae*. Physiol. Plant. **76**:155–163.
16. **Huynh, T. V., D. Dahlbeck, and B. J. Staskawicz.** 1989. Bacterial blight of soybean: regulation of a pathogen gene determining host cultivar specificity. Science **245**:1374–1377.
17. **Ish-Horowicz, D., and J. F. Burke.** 1981. Rapid and efficient cosmid cloning. Nucleic Acids Res. **9**:2989–2998.
18. **Kado, C. I., and S. T. Liu.** 1981. Rapid procedure for detection and isolation of large and small plasmids. J. Bacteriol. **145**:1365–1373.
19. **King, E. O., M. K. Wood, and D. E. Raney.** 1954. Two simple media for the demonstration of pyocyanin and fluorescein. J. Lab. Clin. Med. **44**:301–307.
20. **Klement, Z.** 1982. Hypersensitivity, p. 149–177. *In* M. S. Mount and G. H. Lacy (ed.), Phytopathogenic procaryotes, vol. 2. Academic Press, Inc., New York.
21. **Lindgren, P. B.** 1987. Ph.D. thesis. University of California, Berkeley.
22. **Lindgren, P. B., R. Frederick, A. G. Govindarajan, N. J. Panopoulos, B. J. Staskawicz, and S. E. Lindow.** 1989. An ice nucleation reporter gene system: identification of inducible pathogenicity genes in *Pseudomonas syringae* pv. *phaseolicola*. EMBO J. **8**:2990–3001.
23. **Lindgren, P. B., N. J. Panopoulos, B. J. Staskawicz, and D. Dahlbeck.** 1988. Genes required for pathogenicity and hypersensitivity are conserved and interchangeable among pathovars of *Pseudomonas syringae*. Mol. Gen. Genet. **21**:499–506.
24. **Lindgren, P. B., R. C. Peet, and N. J. Panopoulos.** 1986. Gene cluster of *Pseudomonas syringae* pv. "*phaseolicola*" controls pathogenicity on bean plants and hypersensitivity on nonhost plants. J. Bacteriol. **168**:512–522.
25. **Malick, A. N., A. Vivian, and J. D. Taylor.** 1987. Isolation and partial characterization of three classes of mutant *Pseudomonas syringae* pathovar *pisi*. J. Gen. Microbiol. **133**:2393–2399.
26. **Maniatis, T., E. F. Fritsch, and J. Sambrook.** 1982. Molecular cloning: a laboratory manual. Cold Spring Harbor Laboratory, Cold Spring Harbor, N.Y.
27. **Martinez, E., D. Romero, and R. Palacios.** 1990. The *Rhizobium* genome. Crit. Rev. Plant Sci. **9**:59–93.
28. **Miller, J. H.** 1972. Experiments in molecular genetics. Cold Spring Harbor Laboratory, Cold Spring Harbor, N.Y.
29. **Mills, D., and P. Mukhopadhyay.** 1990. Organization of the *hrpM* locus of *Pseudomonas syringae* pv. *syringae* and its potential function in pathogenesis, p. 47–57. *In* S. Silver, A. M. Chakrabarty, B. Iglewski, and S. Kaplan (ed.), *Pseudomonas*: biotransformations, pathogenesis, and evolving biotechnology. American Society for Microbiology, Washington, D.C.
30. **Mindrinos, M. N., L. G. Rahme, R. T. Frederick, E. Hatziloukas, C. Grimm, and N. J. Panopoulos.** 1990. Structure, function, regulation, and evolution of genes involved in pathogenicity, the hypersensitive response, and phaseolotoxin immunity in the bean halo blight pathogen, p. 74–81. *In* S. Silver, A. M. Chakrabarty, B. Iglewski, and S. Kaplan (ed.), *Pseudomonas*: biotransformations, pathogenesis, and evolving biotechnology. American Society for Microbiology, Washington, D.C.
31. **Mukhopadhyay, P., J. Williams, and D. Mills.** 1988. Molecular analysis of a pathogenicity locus in *Pseudomonas syringae* pv. *syringae*. J. Bacteriol. **170**:5479–5488.
32. **Nester, E. W., M. P. Gordon, R. M. Amasino, and M. F. Yanofsky.** 1984. Crown gall: a molecular and physiological analysis. Annu. Rev. Plant Physiol. **35**:387–413.
33. **Niepold, F., D. Anderson, and D. Mills.** 1985. Cloning determinants of pathogenesis from *Pseudomonas syringae* pathovar *syringae*. Proc. Natl. Acad. Sci. USA **82**:406–410.

33a. **Panopoulos, N. J.** Unpublished data.

34. **Panopoulos, N. J., and R. C. Peet.** 1985. The molecular genetics and plasmids of plant pathogenic bacteria. Annu. Rev. Phytopathol. **23**:381–419.
35. **Peet, R. C., P. B. Lindgren, D. K. Willis, and N. J. Panopoulos.** 1986. Identification and cloning of genes involved in phaseolotoxin production by *Pseudomonas syringae* pv. "*phaseolicola*." J. Bacteriol. **166**:1096–1105.
36. **Rahme, L., M. Mindrinos, C. Grimm, R. Frederick, P. Lindgren, and N. J. Panopoulos.** 1989. Organization and expression of the *hrp* gene cluster of *Pseudomonas syringae* pv. *phaseolicola*, p. 303–314. *In* E. Tjamos and C. Beckman (ed.), Vascular wilt diseases of plants: basic studies and control. Springer-Verlag, New York.

36a. **Rahme, L. G., M. N. Mindrinos, and N. J. Panopoulos.** Unpublished data.

37. **Salch, Y. P., and P. D. Shaw.** 1988. Isolation and characterization of pathogenicity genes of *Pseudomonas syringae* pv. *tabaci*. J. Bacteriol. **170**:2584–2591.
38. **Schroth, M. N., D. C. Hildebrand, and N. J. Panopoulos.** *In* The prokaryotes, 2nd ed., in press. Springer-Verlag, New York.

39. **Somlyai, G., M. Hevesi, Z. Banfalvi, Z. Klement, and A. Kondorosi.** 1986. Isolation and characterization of non-pathogenic and reduced virulence mutants of *Pseudomonas syringae* p. *phaseolicola* induced by Tn*5* transposon insertions. Physiol. Mol. Plant Pathol. **29**:369–380.
40. **Southworth, M. W., P. K. Wolber, and G. J. Warren.** 1988. Nonlinear relationship between concentration and activity of a bacterial ice nucleation protein. J. Biol. Chem. **263**:15211–15216.
41. **Stachel, S. E., G. An, C. Flores, and E. W. Nester.** 1985. A Tn*3* *lacZ* transposon for the random generation of β-galactosidase gene fusions: application to the analysis of gene expression in *Agrobacterium*. EMBO J. **4**:891–898.
42. **Stahl, R. E., and G. V. Minsavage.** 1990. *In* Proceedings of the 7th International Congress on Plant Pathogenic Bacteria, in press. Hungarian Academy of Science, Budapest.
43. **Staskawicz, B., D. Dahlbeck, N. Keen, and C. Napoli.** 1987. Molecular characterization of cloned avirulence genes from race 0 and race 1 of *Pseudomonas syringae* pv. *glycinea*. J. Bacteriol. **169**:5789–5794.
44. **Steinberger, E. M., and S. V. Beer.** 1988. Creation and complementation of pathogenicity mutants of *Erwinia amylovora*. Mol. Plant-Microbe Interact. **1**:135–144.
45. **Vanneste, J. L., J.-P. Paulin, and D. Expert.** 1990. Bacteriophage Mu as a tool to study *Erwinia amylovora* pathogenicity and hypersensitive reaction on tobacco. J. Bacteriol. **172**:932–941.

45a. **Xiao, Y., Y. Lu, and S. W. Hutcheson.** 1990. Abstr. 5th Int. Symp. Mol. Genet. Plant-Microbe Interact., P87, p. 77.

46. **Xu, P., S. Leong, and L. Sequeira.** 1988. Molecular cloning of genes that specify virulence in *Pseudomonas solanacearum*. J. Bacteriol. **170**:617–622.
47. **Yucel, I., Y. Xiao, and S. W. Hutcheson.** 1989. Influence of *Pseudomonas syringae* culture conditions on initiation of the hypersensitive response of cultured tobacco cells. Appl. Environ. Microbiol. **55**:1724–1729.